Journal of the European Ceramic Society **10** (1992) 399–403

Mullite Materials from a 3:2 Alumina–Silica Gel Part II: Microstructural Evolution

M. I. Osendi, C. Baudín & S. de Aza

Instituto de Cerámica y Vidrio, CSIC, E-28500 Arganda del Rey, Madrid, Spain

(Received 11 October 1991; revised version received 13 January 1992; accepted 24 January 1992)

Abstract

The microstructures of mullite materials obtained from amorphous mullite precursors have been determined as a function of the firing cycles. Firing cycles with two isothermal steps have been investigated. Grain size distributions and homogeneity of the final microstructure were very dependent on the temperature of the low isothermal step included in the firing cycle.

Das Gefüge von Mullit-Werkstoffen, die aus amorphen Mullit-Prekursoren hergestellt wurden, ist in Abhängigkeit der Brennzyklen untersucht worden. Die Korngrößenverteilung und die Homogenität des Endgefüges sind deutlich abhängig von der Temperatur des niederen isothermen Brennschrittes, der im Brennzyklus enthalten ist.

Les microstructures de matériaux à base de mullite obtenus à partir de précurseurs amorphes ont été déterminées en fonction du nombre de cycles de pyrolyse. Des cycles de pyrolyse avec deux plateaux isothermes ont été essayés. La distribution de la taille des grains et l'homogénéité de la microstructure finale dépendent beaucoup de la température du plateau isotherme à basse température inclus dans le cycle de pyrolyse.

1 Introduction

It is generally accepted that the microstructure of the mullite bodies obtained from sol–gel precursors strongly depends upon the alumina:silica ratio, mullite grains being fine and equiaxial only for alumina contents exceeding 74 wt%,[1] but acicular for lower alumina contents.[1–3] However, little attention has been paid to the effect of the sintering schedule at low temperatures on microstructural development. In this work, the relationships between sintering schedules and microstructures of mullite materials obtained from an alumina–silica gel with the stoichiometric composition of 3:2 mullite are discussed.

2 Experimental

The powders used and the green compact processing were the same as those described in Part I.[4]

The dynamic sintering curve was obtained in a linear variation of differential transducer (LVDT) dilatometer using the following heating rates: 120°C/h up to 600°C and 240°C/h up to 1550°C.

Three different sintering cycles were used at these heating rates, but adding two isothermal steps. The temperature of one was fixed at 1650°C for 2 h, and different temperatures were tested for the lower isothermal step: 1210, 1250 and 1500°C for 4 h. These temperatures were not chosen arbitrarily but are related to the mullite formation temperature ($\approx$1250°C). Subsequently, annealing treatments at 1650°C for 2 h were performed in the samples.

Microstructures of the sintered bodies were observed by scanning electron microscopy (SEM) on polished and thermally etched surfaces. Microstructures were quantified using the micrographs and a semi-automatic image analyzer. Particle size distributions were obtained considering the equivalent spherical diameter (d), with an average of 500 grains being counted for each sample and 30 classes, between d_{max} and d_{min}, being formed.

Journal of the European Ceramic Society 0955-2219/92/$5.00

3 Results

In Fig. 1 the dynamic sintering curve is depicted. It shows three clearly differentiated zones:

(i) A large shrinkage (≈25%) takes place in a very narrow range of temperatures, from 1100 to 1250°C, with a maximum in the shrinkage rate located at ≈1200°C;
(ii) between 1250 and 1400°C shrinkage is almost arrested; and
(iii) from 1400°C shrinkage proceeds at a lower rate than in (i).

In Fig. 2, the microstructures of mullite bodies for the three sintering cycles described previously are shown. The sample presents exaggerated grain growth and a large number of entrapped alumina grains (Fig. 2(a)) when the low temperature step used was 1210°C. The microstructures are very similar for the two other sintering cycles (Fig. 2(b) and (c)), showing smaller grain sizes than the previous one, with no small alumina particles being detected. In Fig. 3 the microstructures of annealed samples are shown.

In Fig. 4 the particle size distributions of samples treated at 1650°C/2 h are represented for the three cycles. Table 1 summarizes the main characteristics of the particle size distributions for all the samples. The significant width of the distributions was estimated considering only the classes with more than 5% particles. Accordingly, the distributions are centered in the intervals 0·5–1·3 μm, 0·3–0·9 μm and 0·3–0·7, for the samples with the low temperature step at 1210°C, 1250°C and 1500°C, respectively (Fig. 4).

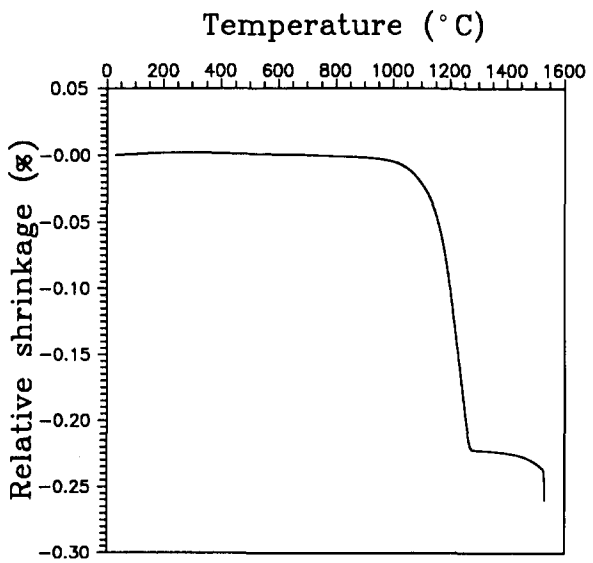

Fig. 1. Relative shrinkage versus temperature. The last straight portion of the curve corresponds to the 1 h isotherm.

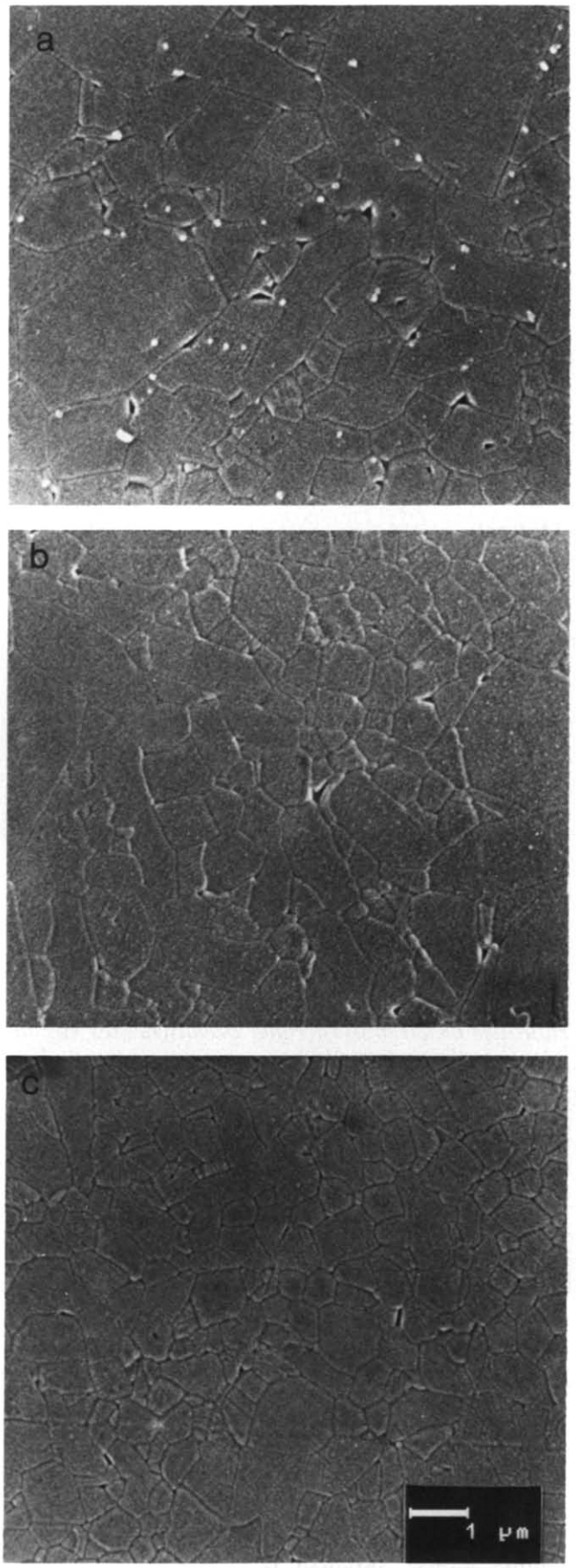

Fig. 2. SEM micrographs of compacts sintered at 1650°C for 2 h and with the low temperature step at (a) 1210°C, (b) 1250°C and (c) 1500°C.

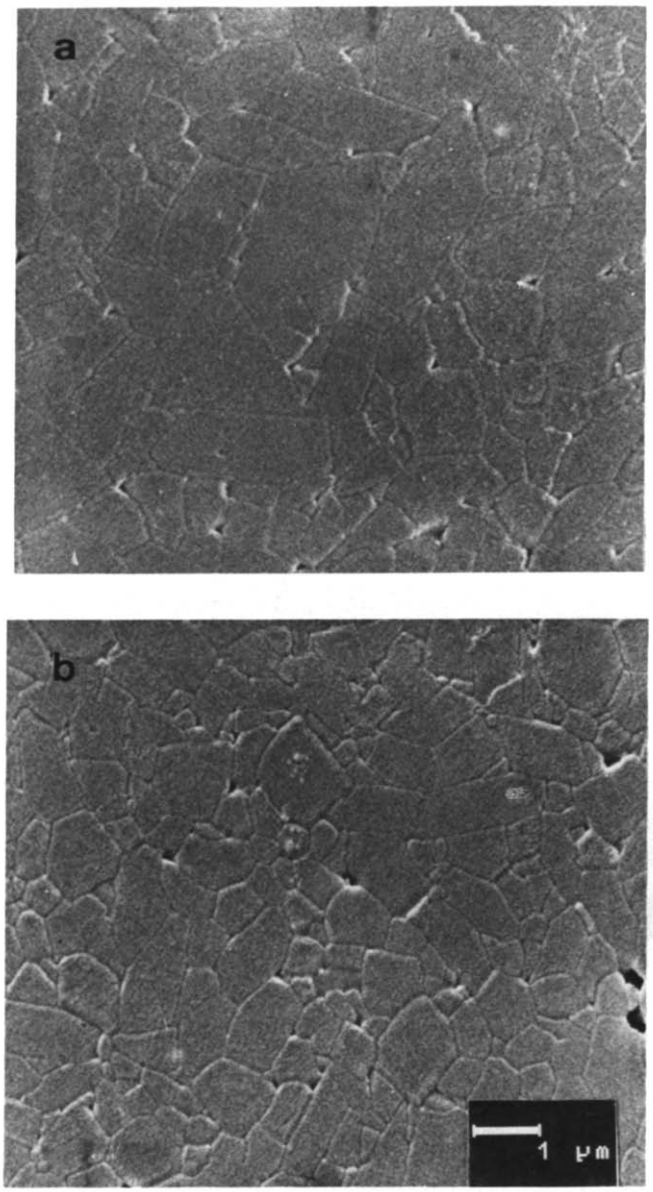

Fig. 3. SEM micrographs of compacts sintered at 1650°C for 4 h and with the low temperature step at (a) 1250°C and (b) 1500°C.

Table 1. Characteristics of grain size distributions

Thermal treatment	*Average diameter* (μm)	*Number of particles (%)*		*Distribution width* (μm)
		$G < 0{\cdot}5\ \mu m$	$G > 1\ \mu m$	
1210°C/4 h 1650°C/2 h	0·9	24	24	0·8
1250°C/4 h 1650°C/2 h	0·7	40	12	0·6
1500°C/4 h 1650°C/2 h	0·6	60	4	0·5
1250°C/4 h 1650°C/4 h	0·8	24	16	0·7
1500°C/4 h 1650°C/4 h	0·7	38	10	0·6

It is clear that the grain size distribution for the sample sintered using a low temperature isotherm at 1210°C was the widest (0·8 μm) and that it is centered over the largest grain sizes (Fig. 4). Conversely, the grain size distribution of the sample obtained with the low temperature isotherm at 1500°C is narrower (0·6 μm) and shows smaller grain sizes (Fig. 4). This shift towards lower particle sizes as the low temperature isotherm increases is obvious when observing the cumulative frequency curves (Fig. 5). Annealing treatments of 2 h at 1650°C widen the particle size distributions and average grain sizes are slightly increased (Table 1).

4 Discussion

The fast shrinkage rate that shows the sintering curve (Fig. 1) in the 1100–1250°C interval corresponds to viscous flow sintering, as has already been proposed for the sintering of compacts made of sol–gel precursors.[5–7] Once mullite is nucleated ($T = 1250$°C), this phenomenon is arrested and mainly solid-state sintering follows between mullite grains at $T > 1400$°C.

The exaggerated growth of the mullite grains when the low temperature sintering step takes place at 1210°C (Table 1, Figs 2(a), 4(a) and 5(a)) can be partially explained by the viscous flow sintering mechanism at temperatures under that of mullite formation ($T \approx 1250$°C). Conversely. the microstructures of the mullite bodies obtained using low temperature steps at 1250 and 1500°C are more regular and exaggerated grain growth is inhibited (Table 1, Figs 2(b) and (c), 4(b) and (c), 5(b) and (c)).

Observations by TEM and EDX on the powders have shown[7] the existence of small alumina particles ($\approx$ nm) in the gel treated at $T < 1300$°C. These particles act as seeds for α-Al_2O_3 formation at the bohemite–α-alumina transition at $T > 1200$°C,[8] leading to alumina grain growth. This is the case for the compacts treated using 1210°C as the low temperature step in which alumina particles are clearly observed (Fig. 2(a)). Therefore, sintering cycles with isothermal steps below the mullite formation temperature can produce phase segregation, especially if the initial powders are not completely homogeneous, as is the case for the colloidal-type gels.[9]

Alumina growth at low temperatures decompensates the overall $3Al_2O_3{:}2SiO_2$ initial composition of the gel. Thus, a silica-rich glassy phase exists, which will enhance grain growth by liquid-phase sintering during the firing step at 1650°C. This fact is also responsible for the exaggerated grain growth

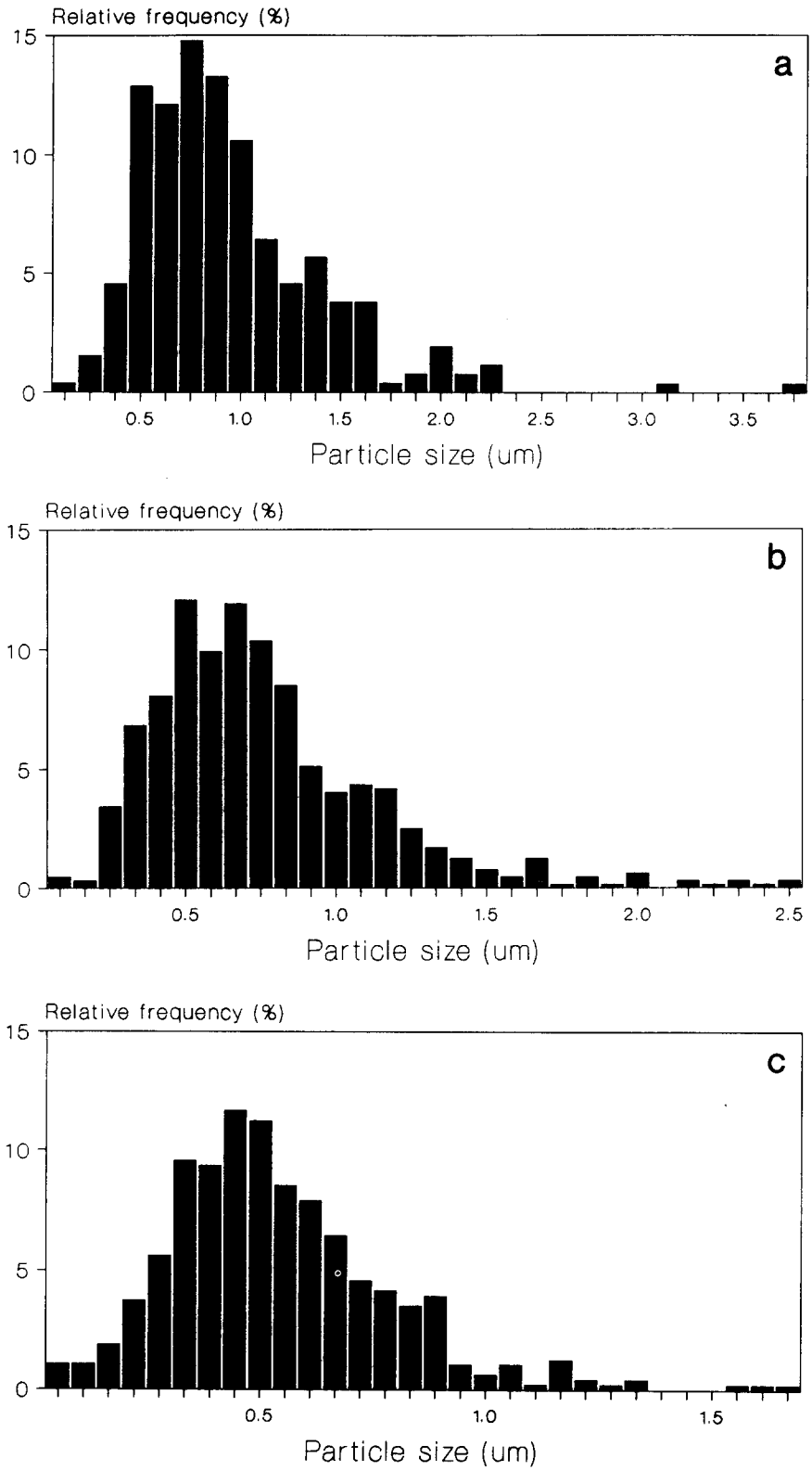

Fig. 4. Particle size distributions of samples sintered at 1650°C/2 h and with the low temperature step at (a) 1210°C, (b) 1250°C and (c) 1500°C.

that takes place in the compacts treated using 1210°C as the low temperature step (Table 1, Figs 2(a), 4(a) and 5(a)).

No liquid-phase sintering at 1650°C is expected in the samples fired using 1250 and 1500°C as low temperature steps. In fact, fine and homogeneous microstructures are obtained, and even the annealing treatments at 1650°C do not produce significant grain growth (Table 1, Fig. 3).

These results show the importance of the thermal cycles selected to sinter these kinds of gels. Depending on the low temperature step, microstructures

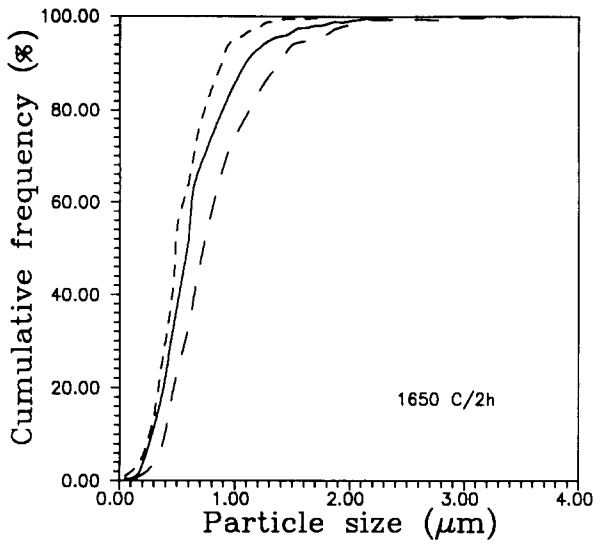

Fig. 5. Cumulative frequency curves as a function of grain size for the three sintering cycles with annealing treatment at 1650°C/2 h. The corresponding low-temperature isothermal steps are: 1210°C (– – –), 1250°C (——) and 1500°C (– – – –).

with exaggerated grain growth and phase segregation or with a narrow and small grain size distribution and compositionally homogeneous may be obtained (Figs 2 and 5). This specific behavior allows the selection of the microstructure more appropriate to the final requirements.

The particular development of the microstructure of the gel as a function of the sintering schedule is a direct consequence of the fact that the initial powder has been treated at a temperature (1000°C) where no mullite nucleation occurs. If the gel were initially treated at a temperature where mullite formation takes place, its microstructure would evolve differently. Therefore, initial treatment of the gel at temperatures below that of mullite formation not only favors sintering[4] but also allows manipulation of the microstructure as sintering and reaction are taking place during the firing cycle.

5 Conclusions

Final microstructures of mullite materials obtained from chemical precursors can be strongly modified according to the thermal cycle designed to sinter the compacts. If the sintering curve has isothermal treatments at temperatures below that corresponding to mullite nucleation, exaggerated grain growth together with unreacted alumina particles are observed in the microstructure of the fired mullite materials. For sintering schedules with isothermal treatments above the temperature of mullite formation, the microstructures show narrower grain size distributions with a smaller average grain size.

Acknowledgement

This research was supported by CICYT (Spain), Program No. MAT88-0182.

References

1. Kanzaki, S., Tabata, H. & Kumazawa, T., Sintering and mechanical properties of mullite derived via spray pyrolysis. In *Mullite and Mullite Matrix Composites, Ceramic Transactions*, Vol. 6, ed. S. Somiya, R. F. Davis & J. A. Pask. The American Ceramic Society, OH, 1990, pp. 339–51.
2. Kumazawa, T., Ohta, S., Kanzaki, S. & Tabata, H., Influence of powder characteristics on microstructure and mechanical properties of mullite ceramics. In *Mullite and Mullite Matrix Composites, Ceramic Transactions*, Vol. 6, ed. S. Somiya, R. F. Davis & J. A. Pask. The American Ceramic Society, OH, 1990, pp. 401–11.
3. Mizuno, M., Shiraishi, M. & Saito, H., Microstructure and bending strength of highly pure mullite ceramics. In *Mullite and Mullite Matrix Composites, Ceramic Transactions*, Vol. 6, ed. S. Somiya, R. F. Davis & J. A. Pask. The American Ceramic Society, OH, 1990, pp. 413–24.
4. Baudín, C., Osendi, M. I. & de Aza, S., Mullite materials from a 3:2 alumina–silica gel. Part I: Green processing and porosity. *J. Eur. Ceram. Soc.*, **10** (1992) 393–8.
5. Binker, C. J. & Scherer, G. W., Theories of viscous sintering. In *Sol–Gel Science*, ed. Academic Press, London, UK, 1980, pp. 675–730.
6. Hirata, Y., Sakeda, K., Matshushita, Y., Shimada, K. & Ishihara, Y., Characterization and sintering behavior of alkoxide-derived aluminosilicate powders. *J. Am. Ceram. Soc.*, **72** (1989) 995–1002.
7. Osendi, M. I., Baudín, C., de Aza, S. & Moya, J. S., Processing and sintering of a 3:2 alumina/silica gel. *Ceram. Int.*, in press.
8. Roy, R., A strategy for research on synthesis of ceramic materials. In *Advanced Ceramics III*, ed. S. Somiya. Elsevier Applied Science, London, 1990, pp. 1–23.
9. Yoldas, B. E., Mullite formation from aluminum and silicon alkoxides. In *Mullite and Mullite Matrix Composites, Ceramic Transactions*, Vol. 6, ed. S. Somiya, R. F. Davis & J. A. Pask. The American Ceramic Society, OH, 1990, pp. 255–61.